Printed in U.S.A.

75-GT-121

an ASME publication

$3.00 PER COPY
$1.00 TO ASME MEMBERS

A General Finite Difference Technique for the Compressible Flow in the Meridional Plane of Centrifugal Turbomachinery

W. R. DAVIS

Mechanical Engineer,
Research Division,
Carrier Corp.,
Syracuse, N. Y.

There has been an increased concentration of effort recently in the understanding of the complex flow in centrifugal turbomachines, especially industrial machines. Although it is impossible at this time, to model all the phenomena existing in a real machine, it is felt that a systematic approach which makes use of recent advances in computational fluid dynamics, and extends these as further developments occur, will significantly improve our understanding of the flow, and our ability to predict performance and improve efficiency. In this paper, a new general finite difference technique for solving the flow field in the hub-to-shroud plane of any component of a centrifugal turbomachine is described. The technique uses a quasi-orthogonal finite-difference net, and solves the resulting system of equations using a matrix method. Thus the technique offers a stable, accurate computational method, combined with a fixed grid which may be simply applied to the most complex annular passage shape. The results for three numerical examples are presented, a radial to axial inlet, a vaneless radial diffuser and an interstage return bend.

Contributed by the Gas Turbine Division of The American Society of Mechanical Engineers for presentation at the Gas Turbine Conference & Products Show, Houston, Texas, March 2-6, 1975. Manuscript received at ASME Headquarters December 13, 1974.

Copies will be available until December 1, 1975.

A General Finite Difference Technique for the Compressible Flow in the Meridional Plane of Centrifugal Turbomachinery

W. R. DAVIS

INTRODUCTION

The demand for increased efficiency and accurate performance predictions, in the area of industrial centrifugal turbomachinery, has recently received considerable attention. One result has been an increased concentration of effort in the understanding of the complex flow in centrifugal machines. It appears that relatively recent advances in computational fluid dynamics may prove valuable when applied in this area. For example, Senoo (1)[1] and Novak (2) have used the streamline curvature method to solve the flow field in the meridional plane of a centrifugal impeller.

More traditional potential flow solutions, e.g., the work of Stanitz (3), do not have the flexibility of the foregoing work. Another approach is to use empirical design methods based on large amounts of data, which treat essentially the inlet and exit conditions. Jansen (4) considered the flow in a vaneless radial diffuser, assumed that both wall boundary layers were identical, and then solved a special case of the three-dimensional turbulent boundary-layer equations.

It must be recognized that the flow in a centrifugal machine is extremely complex, as pointed out by Dean (5). Although it is impossible at this time to model all the phenomena existing in a real machine, it is felt that a systematic approach, which begins with state-of-the-art analytical techniques in fluid dynamics, and extends these as further developments occur, will significantly improve both our understanding of flow and our ability to predict performance and improve efficiency.

One approach would be to attempt the solution of the complete Navier Stokes Equations, but this is such a formidable problem as to be out of reach now and in the immediate future. Another approach is to assume that a two-layer model is representative, i.e., an inviscid flow solution which interacts with an end wall boundary-layer calculation. In this way, the model is flexible and can be altered to include separation zones and skewed boundary layers if necessary. This method is feasible at the present time.

In Reference (6), Wu presents a rigorous derivation of the equations which govern the inviscid flow on two intersecting families of stream surfaces, which he called surfaces of the first and second kind. These S_1 and S_2 surfaces are general stream surfaces, more commonly known as the blade-to-blade surface and hub-to-shroud surface, respectively, and are not restricted, as is commonly done, to the simpler surface of revolution (S_1) and a surface made up of radial elements (S_2). Instead, they are allowed freedom to warp as a function of the computed flow field, and thus the complete three-dimensional solution requires an iterative technique, with information being fed from one surface to the other until a stable converged solution is obtained. Wu (6) also suggested a finite-difference approach for the solution of the flow field on both surfaces, which would generate a set of non-linear equations which could then be solved using either an iterative matrix technique or a relaxation procedure.

More recently, Marsh (7), using the Wu approach, employed an irregular finite-difference net on the S_2 surface, to generate the set of non-linear equations, which he then solved using an iterative matrix approach. The importance of this irregular net is that the boundary grid points fall on the physical boundaries of the machine, even when the boundaries are curved, as they generally are in modern turbomachines, Fig. 1(b).

Smith and Frost (8) successfully extended the Marsh/Wu technique to the S_1 (blade-to-blade)

[1] Underlined numbers in parentheses designate References at end of paper.

NOMENCLATURE

a_i, b_i, c_i = finite difference coefficients used to multiply the function value at a stencil point

$[A]$ = coefficient matrix of the principle equation, equation (8)

b = integrating factor for the continuity equation, or the stream sheet thickness

$\bar{F}$ = vector, parallel to $\bar{n}$, due to tangential gradients (units of force per unit mass)

f = any two-dimensional function

h = static enthalpy per unit mass of fluid

I = rothalpy ($H_o - \omega RV_\theta$)

$[L]$ = lower triangular banded coefficient matrix

m = meridional direction, or the streamline direction in the meridional plane

M = Mach number

m = number of quasi-orthogonals

n = number of grid points across the annulus (quasi-streamlines)

$\bar{n}$ = unit vector normal to relative stream surface S_2

p = static pressure

q = any quantity on relative stream surface S_2

$[Q], q$ = vector on the right-hand side of the principal equation

R = radius

R_g = gas constant

s = entropy per unit mass

S_1 = relative stream surface passing through fluid particles in the circumferential plane

S_2 = relative stream surface passing through fluid particles in the meridional plane

T = static temperature

t = time

$[U]$ = upper triangular banded coefficient matrix

$\bar{V}$ = absolute velocity vector

$\bar{W}$ = relative velocity vector

z = axial direction

α = finite difference operator for the operator $\nabla^2( )$

$\beta; \kappa$ = finite difference operators for partials f_R and f_z

β = flow angle measured from the meridional direction

ξ = function on the right hand side of the principal equation

ρ = fluid density

θ = tangential direction

θ = angle between the R, z and x,y coordinate systems

ψ = stream function defined on relative stream surface S_2

$[\psi]$ = column vector of ψ

$\bar{\omega}$ = angular velocity of the relative coordinate system

$\frac{\partial f}{\partial R}$, f_R = partial derivatives of f with respect to R

$\nabla^2( )$ = the operator ($f_{RR} + f_{zz}$)

$D( )/Dt$ = total or substantial derivative

Subscripts

i = grid point subscript (across the annulus)

j = grid point subscript (along the annulus)

m = meridional component

o = total state

R, θ, Z = radial, tangential, and axial components

surface, employing the governing equations derived by Wu, the irregular finite-difference grid developed by Marsh, and the appropriate boundary conditions for the regions upstream and downstream of the cascade.

The author has successfully implemented the Marsh technique and the more familiar streamline curvature method for the inviscid flow on the S_2 surface of axial flow compressors (9, 10), as part of axial compressor performance prediction computer programs developed at Carleton University. Also, a matrix technique, similar to that described by Smith (8) was used in a computer program which computes the flow field on the S_1 surface (11). This experience with the matrix technique indicated that it is a stable, accurate, inviscid flow computation technique which offers some advantages over the more commonly used streamline curvature method (12).

Some comment on the disadvantages of the streamline curvature method is in order, since the quasi-orthogonal streamline curvature method used by Senoo (1) and Novak (2), does appear to be attractive. The accurate calculation of the streamline curvature has always been a source of trouble in this method, and great care must be taken to avoid instabilities which may cause divergence of the solution. Wilkinson (13) investigated this problem for very small values of curvature and recommended optimum procedures

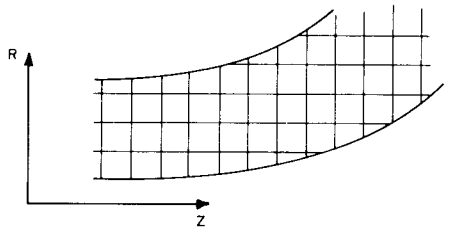

(a) Regular or rectangular net

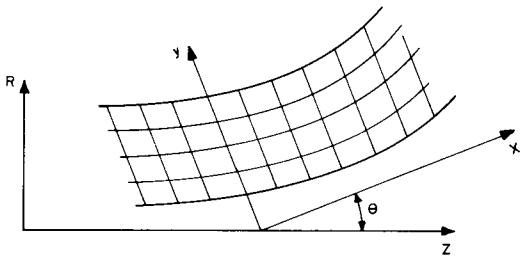

(b) Irregular parallel net (Marsh)

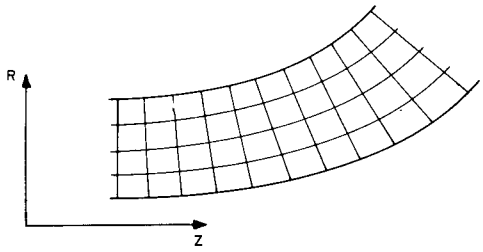

(c) Irregular quasi-orthogonal net

Fig. 1 Finite difference grids

which were significantly different than the conventional methods which are used. A similar study has not been reported for the severe curvatures encountered in some centrifugal machine components. In Reference (12), Davis and Millar compared the streamline curvature and matrix methods as they were applied to the analysis of flow in axial turbomachinery. It was concluded that there was some advantage to the matrix method, mainly due to stability considerations. Further comparisons have been carried out for the geometries considered in this paper with similar conclusions. The streamline curvature method also requires a number of coordinate transformations, since in a cylindrical coordinate system, the streamline slopes become infinite in certain components, and similarly, streamline curvatures are not defined. The inherent instability of the technique requires that streamline shifts be damped, and it follows that any addition to the analytical model which interacts with the streamline position, such as a boundary-layer calculation, will be a potential source of instability. It should also be noted that the streamline slopes and curvatures must be recomputed every time the streamline position changes, i.e., each iteration.

Both Marsh and Smith, using the matrix techniques described in the foregoing, wrote the governing equation in a coordinate system rotated through an angle from the axial direction, as shown in Fig. 1(b), in order to extend the application of their procedures to a wider range of turbomachines.

However, in the area of centrifugal turbomachines, especially multi-stage machines, when considering the flow on the S_2 surface, the designer is confronted with a series of 90- and 180-bends with, in some cases, extreme curvatures and rates of change of curvature. The application of a Marsh type of grid to centrifugal machinery components is very difficult in most cases, due to the proximity of the components and impossible in other cases, for example, an interstage return bend (180-deg annular bend). However, since the finite-difference approach has demonstrated reliability, accuracy, and stability, all of which are important when considering the complex flow in centrifugal passages, it is desirable to use this approach.

The foregoing discussion suggests that a technique which uses the fixed grid approach of Wu (6) or Marsh (7), and yet has the flexibility of the quasi-orthogonal grid, would be well suited to the flow problems encountered in centrifugal turbomachinery. For these reasons, the author has developed a general finite-difference technique which uses a curvilinear grid to solve the inviscid compressible flow on the S_2 (hub-to-shroud) surface of any turbomachinery component or components. The grid, as shown in Fig. 1(c), is made up of arbitrary quasi-orthogonals, and quasi-streamlines spaced at equal intervals between the boundaries. Since streamline curvatures and slopes are not required, any arbitrary duct geometry may be considered without additional difficulty. At the same time, the stability and accuracy of the matrix technique is retained.

Although the examples discussed in this paper do not include any rotating components, such as an impeller, the technique is not limited to stationary components. The omission is deliberate since additional analytical models for rotating three-dimensional boundary layers, separation zones, and circumferential variations, among others, are required before any meaningful comparisons with data could be presented. As reliable models in these areas are developed, they can be combined with the inviscid technique described herein.

The paper describes the development of the quasi-orthogonal, finite-difference technique

in the foregoing, and its application to the flow in the hub-to-shroud plane of turbomachinery. The governing flow equations and the procedure of solution are described. The finite-difference procedure and a turbulent boundary-layer calculation technique have been implemented in a computer program, and the results for a radial to axial inlet, a radial diffuser, and an interstage return bend are presented.

MATHEMATICAL ANALYSIS

The derivation of the equations governing the inviscid compressible flow on an S_2 surface in this paper is similar to the development of Wu (6) and, therefore, is given in the Appendix. These equations, for adiabatic flow, are summarized as follows.

The energy equation is given by,

$$T \frac{Ds}{Dt} = Q = 0, \tag{1}$$

where the operator, D ( )/Dt, indicates a total derivative, or for steady flow, the derivative along a streamline.

The equation of state for a perfect gas may be written

$$P = \rho R_g T . \tag{2}$$

The orthogonality relation for the body force from the equations of motion, and the S_2 stream surface is given as,

$$\bar{F} \cdot \bar{W} = 0 . \tag{3}$$

By the use of equation (3), and the equations of motion in cylindrical coordinates, we have

$$\frac{DI}{Dt} = T \frac{Ds}{Dt} = 0 . \tag{4}$$

The circumferential component of the equation of motion may be written

$$\frac{1}{R} \frac{D(RV_\theta)}{Dt} = F_\theta , \tag{5}$$

where F_θ is the tangential component of the force vector defined by

$$\bar{F} = - \frac{1}{n_\theta R} \left[\frac{\partial h}{\partial \theta} - T \frac{\partial s}{\partial \theta} \right] \bar{n} . \tag{6}$$

The stream function is derived from the continuity equation, and may be defined as

$$\frac{\partial \psi}{\partial R} = \rho b R W_z , \tag{7a}$$

$$\frac{\partial \psi}{\partial Z} = - \rho b R W_R . \tag{7b}$$

where Rb may be thought of as the thickness of the stream surface in the tangential direction.

If equation (7) is substituted into the radial and axial components of the equation of motion written on an S_2 stream surface, we obtain two equations which are very similar in form, and for conciseness may be written

$$\frac{\partial^2 \psi}{\partial R^2} + \frac{\partial^2 \psi}{\partial z^2} = q \left(R, z, \frac{\partial \psi}{\partial R}, \frac{\partial \psi}{\partial z} \right) + \xi_i , \quad \text{for } i = 1,2 \tag{8}$$

where

$$q = \frac{\partial \psi}{\partial R} \cdot \frac{\partial (\ln R b \rho)}{\partial R} + \frac{\partial \psi}{\partial z} \cdot \frac{\partial (\ln b \rho)}{\partial z} ,$$

$$\xi_1 = \frac{Rb\rho}{W_R} \left[- \frac{\partial I}{\partial R} + T \frac{\partial s}{\partial R} + \frac{W_\theta}{R} \frac{\partial (RV_\theta)}{\partial R} + F_R \right] ,$$

and

$$\xi_2 = \frac{Rb\rho}{W_z} \left[- \frac{\partial I}{\partial z} + T \frac{\partial s}{\partial z} + \frac{W_\theta}{R} \frac{\partial (RV_\theta)}{\partial z} + F_z \right] .$$

Equation (8) is a second-order, non-linear, two-dimensional partial differential equation, called the stream function equation or the principal equation. Equation (8) may be expanded into two principal equations, since ξ_1 corresponds to the radial component, and ξ_2 to the axial component of the equation of motion. Only one of these principal equations is required to solve the system of equations (1) through (8).

Wu (6) and Marsh (7) both use the radial component (i = 1); since F_R is always much smaller than F_Z in axial flow machines, and F_R is zero or nearly zero on S_2 surfaces for mixed flow impellers with radial blade elements.

However, we wish to apply the principal equation in regions where we may have purely radial or axial flow; i.e., W_R or W_Z may in general be zero, and the right-hand side of either equation would not be defined. This complication may be avoided by writing the equations in a streamline coordinate system, but the equations are then dependent on the streamline slope and curvature, and as explained earlier, it is desirable to avoid this dependancy.

Therefore, it is necessary to use the axial version of equation (8) (i = 2), in regions where $W_Z > W_R$, and the radial version of equation (8)

(i = 1) in regions where $W_R > W_Z$.

There are seven independent relations contained in equations (1) to (8), and there are nine unknowns, if we consider b as given; i.e., ψ, W_R, W_Z, W_θ, F_R, F_Z, F_θ, S, and I (or ρ). If the shape of the S_2 surface is assumed to be known, two additional relations between the $\bar{F}$ or $\bar{n}$ components will completely define the problem.

NUMERICAL TECHNIQUE

The previous section has described the governing equations for the inviscid compressible flow on an S_2 surface. These equations form a system of non-linear partial differential equations which, in general, are not soluble unless an approximate numerical technique is employed.

The technique described here concerns the numerical solution of the principal equation, for prescribed boundary conditions, at discrete points in the region of interest. The remaining equations, equations (1) to (7) are used as auxiliary equations to relate properties along the stream function lines computed from equation (8). Since equation (8) is nonlinear, the process is iterative, with the functions, ξ_i and q, assumed known and recomputed each iteration.

If we cover the area of interest with a mesh of grid points, equation (8) can be applied to every grid point, and by replacing the differential operator $\nabla^2(\ )$ by a finite difference operator, a system of algebraic equations in the unknown, ψ, will be built up. This system of equations can be expressed in matrix form as:

$$[A][\psi] = [Q] \tag{9}$$

where $[A]$ is the square coefficient matrix derived from replacing the differential operator $\nabla^2(\ )$, $[\psi]$ is the vector of unknown stream function values and $[Q]$ the vector of quantities q, and the boundary values.

Finite-Difference Approximations

It is necessary to replace the mathematical operator modifying ψ at any point P, by some linear combination of the function values at discrete points in the flow field. If these discrete points lie on a regular grid, then the linear coefficients are simple, well defined, and tabulated in suitable texts. However, to maintain a given order of accuracy for an irregular grid, a large number of coefficients are required, and they will be different (in general) for every point in the grid.

As with most finite-difference methods, the Taylor's series is used to relate the changes

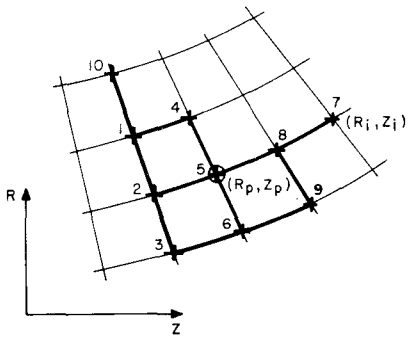

(a) 10-Point stencil for $\nabla^2(\ )$

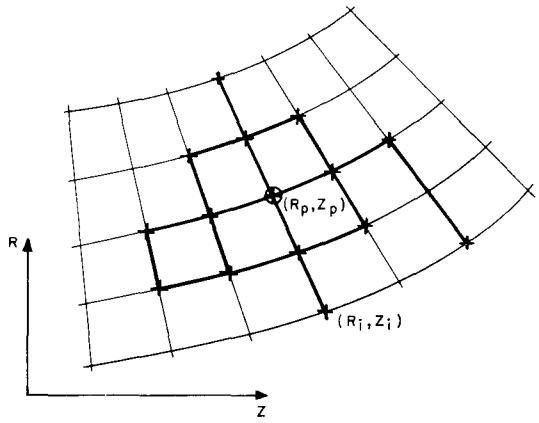

(b) 15-Point stencil for $\partial f/\partial R$, $\partial f/\partial z$

Fig. 2 Finite-difference stencils

over a finite interval in the neighborhood of a point of interest to the values of the function and its derivatives at that point. Any operator, for example $\partial(\ )/\partial Z$ or $\nabla^2(\ )$, can be expressed as a linear combination of the function values at the surrounding points, to a degree of accuracy depending on the number and location of these points. Letting α represent such an operator, this is expressible as:

$$\alpha = \sum_i a_i \, f(R_i, z_i) \tag{10a}$$

where a_i is the coefficient multiplying the function value at the point, i, with coordinates R_i, z_i. The function value, $f(R_1, z_1)$, can be expanded in a two-dimensional Taylor's series around the point of interest (R_p, z_p), and if we substitute in equation (10a) and group terms, we have

$$\alpha = \left(\sum_i a_i\right) f\Big]_p + \left(\sum_i a_i \, \Delta R_i\right) f_R\Big]_p + \left(\sum_i a_i \, \Delta z_i\right) f_z\Big]_p + \cdots \tag{10b}$$

where the subscripts, R and z, denote partial differentiation with respect to R and z. The

Taylor's series must be truncated for practical purposes, the accuracy desired defining the number of terms retained. For example, if third-order accuracy is desired, it can be shown that ten terms must be retained, and in order to solve for the coefficients, we will require ten grid points. Equation (10b) can be broken into as many equations as there are terms in the Taylor's series by equating coefficients of like terms; for the ten terms retained to obtain third-order accuracy, ten equations result, which may be solved for the coefficients, a_i. For example if we have

$$\alpha = \frac{\partial 2\ f}{\partial R^2} + \frac{\partial^2 f}{\partial Z^2}$$

the coefficients of the left-hand side (and thus the right-hand side), of equation (10b) truncated after the tenth term, will all be zero, except for the coefficients of the second derivatives, f_{RR} and f_{zz}.

The foregoing procedure may be made clear by a simple example. Consider the case of a square grid with spacing X in both directions, and assume that the grid points are numbered as shown in Fig. 2(a). Now when the coefficients of ten terms of equation (10b) are expanded for a square grid, and set equal to the Laplacian coefficients, that is unity for the derivatives, f_{RR} and f_{zz}, we have

$$a_1 + a_2 + a_3 + \ldots + a_{10} = 0,$$

$$X(a_1 + a_4) - X(a_3 + a_6 + a_9) + 2a_{10} X = 0,$$

$$- X(a_1 + a_2 + a_3 + a_{10}) + X(a_8 + a_9) + 2a_7 X = 0,$$

and so on, until we have ten equations in the ten unknowns, a_i.

This system of equations can be solved quickly by hand to give

$$a_1 = a_3 = a_9 = a_7 = a_{10} = 0,$$

$$a_2 = a_4 = a_6 = a_8 = X^{-2},$$

$$a_5 = - 4X^{-2}.$$

The finite difference expression for the Laplacian thus reduces to

$$\alpha = \frac{\partial 2\ f}{\partial R^2} + \frac{\partial 2\ f}{\partial Z} \simeq \frac{1}{X^2} (f_2 + f_4 + f_6 + f_8 - 4f_5),$$

where the subscripts refer to the stencil point of Fig. 2(a).

In general, for rectangular grids, if we require third-order accuracy (10 terms), we require information from four grid lines in the R and z direction. That is, the finite-difference stencil must be chosen so that the grid points fall on four grid lines in each direction. If we do not, the ten equations will not be independent.

It is desirable to minimize the number of grid lines which the finite-difference stencil covers since, for practical purposes, one wishes to minimize the width of the banded matrix which results from the system of difference equations. Marsh was able to reduce the number of grid lines required to three and still retain third-order accuracy by an elegant device which made use of the particular geometry of his irregular net. Specifically, the irregular net which he used, was made up of parallel lines in one of the directions (axial), as shown in Fig. 1(b).

Unfortunately, for the quasi-orthogonal grid which is used here, this device is not applicable, and it is necessary to use four grid lines in each direction. The finite difference stencil which has proved to be successful in computing the operator, $\partial^2(\ )/\partial R^2 + \partial^2(\ )/\partial Z^2$, with third-order accuracy is shown in Fig. 2(a).

In order to evaluate the functions, ξ and q, of equation (8), the first derivatives in the axial and radial directions must be computed in a manner similar to that described in the foregoing for the operator $\nabla^2(\ )$. That is, we set:

$$q = \frac{\partial f}{\partial R} = \sum_i b_i f_i ,$$

and

$$\xi = \frac{\partial f}{\partial z} = \sum_i c_i f_i ,$$

and calculate the linear coefficients, b_i and c_i. An interesting result was that for some of the geometries considered, it was necessary to use a fourth-order finite-difference stencil (15 grid points) for the first derivative, to obtain the correct solution of equation (8). Thus, a 15-point stencil covering five grid lines in each direction was employed to compute the coefficient, b_i and c_i. A typical interior grid point stencil is shown in Fig. 3(b).

As can be seen by examining the stencils in Fig. 2, when the point at which the finite-difference coefficients are being computed (R_p, Z_p), is next to a boundary, some of the stencil points will fall outside of the boundary. To avoid this, the stencil is altered sufficiently so that all of the stencil points fall within the region of interest. The change in shapes is generally achieved by moving the stencil point to

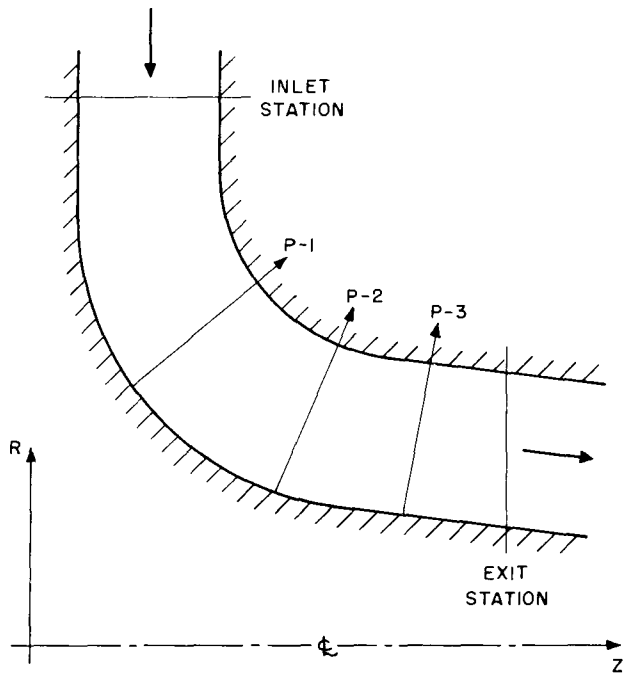

Fig. 3(a) Radial to axial flow inlet

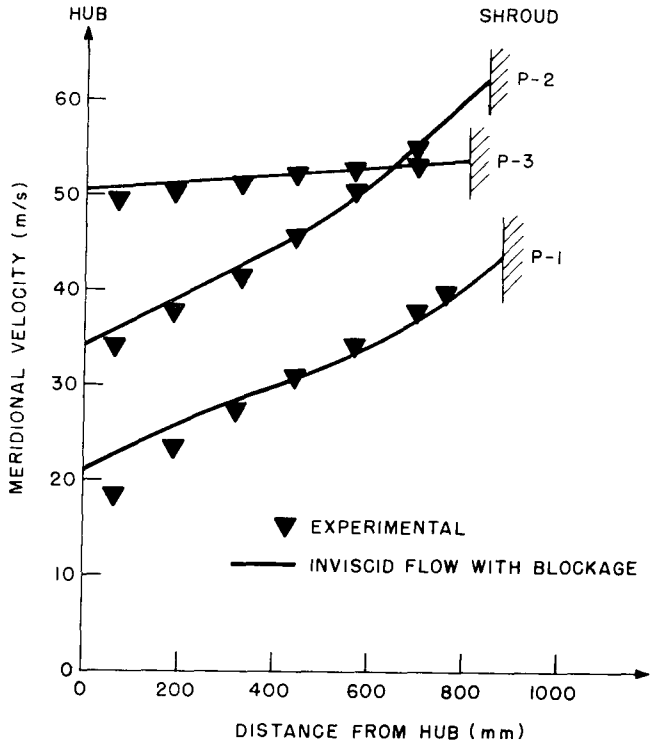

Fig. 3(b) Radial to axial flow inlet velocity profiles

the other side of the stencil. For example, at the exit boundary, point 7 of Fig. 2(a) is placed beside point 2.

Boundary Conditions

In flow along S_2 surfaces, the boundary walls extend from inlet to exit, and if they are solid, the stream function will be constant along each wall. That is, if we define ψ' as the stream function, ψ, non-dimensionalized with respect to mass flow, we have on the hub or inner wall:

$$\psi'_{1,j} = 0 \ ,$$

and on the tip or outer wall:

$$\psi'_{n,j} = 1.0.$$

At the inlet, we may assume that conditions are known, and the variation of ψ' across the annulus on the inlet grid line may be computed.

At the exit station, it is necessary to make some assumption which relates the ψ' values on the exit grid line to those on the adjacent upstream grid line. The assumption made here is that the stream function is constant between these two grid lines. That is,

$$\psi'_{i,m-1} = \psi'_{i,m} \ ,$$

and the location of the exit station should be chosen so that this approximation is reasonable.

Method of Solution

The foregoing finite-difference operators, along with the boundary conditions and an initial guess at the flow properties throughout, result in the matrix equation

$$[A][\psi] = [Q] \ . \qquad (11)$$

$[A]$ is a square banded matrix of band width $(4n-7)$, and since there are (n-2) x (m-2) interior grid points (where m is the number of quasi-orthogonals and n is the number of quasi-streamlines), $[A]$ is a sparse matrix. To minimize computer storage requirements, $[A]$ is factored into an upper and lower triangular banded matrix such that:

$$[A] = [L][U] \qquad (12)$$

and the resulting equation:

$$[L][U][\psi] = [Q] \qquad (13)$$

may be solved explicity for $[\psi]$. This is necessary since the inverse of $[A]$ will not be a banded matrix and core storage requirements would become prohibitive.

For axisymetric flow, equation (5) gives:

$$\frac{1}{R}\frac{d(RV_\theta)}{dm} = 0, \qquad (14)$$

and since from equations (1) and (4):

$$\frac{dI}{dm} = T\frac{ds}{dm} = 0, \qquad (15)$$

once the vector, ψ, has been computed, the properties, I, RV_θ, and s, may be related along streamlines to compute these quantities at each grid point. Note that "m" is the direction of the streamline in the meridional plane and will be referred to as the meridional direction.

The density is allowed to lag one iteration, so that once the velocity components have been computed from equation (7), the density may be computed simply from the equation of state.

In a duct region (no blades), the S_2 surface will be defined by the tangential velocity computed from equation (14), whereas if the surface passes through a blade row, it is necessary to specify the shape of the surface. Currently, the angle that the surface makes with the meridional direction is specified at each station within the blade row. That is,

$$\beta = \tan^{-1}\left(\frac{V_\theta}{V_m}\right) \qquad (16)$$

When the flow properties have been computed at all grid points, the vector $[Q]$ is recalculated, and equation (13) solved again. This process is repeated until the change in the vector $[\psi]$ is within a specified tolerance on successive iterations.

Limitations

The technique as described may be used to compute a true three-dimensional inviscid flow field on an S_2 surface if enough information is available from some other source. Specifically, a geometric description on the S_2 stream sheet and the property gradients in the tangential directions are required, and these, in general, would require the complete solution of the flow on several S_1 stream sheets.

In practice, the shape of the S_2 surface is estimated, and by assuming axisymmetric flow, the tangential gradients are eliminated. If computations within a blade row are required, the shape of the surface is simplified by following a mean stream surface defined by the mean flow angle.

The two-layer approach requires that a reliable end-wall boundary-layer calculation procedure be available if viscous flow situations are to be treated realistically. For two-dimensional and axisymmetric applications, there are many good boundary-layer calculation techniques described in the literature. If three-dimensional effects, such as significant cross-flow in the boundary layer, or separated flow regions are likely to exist, then additional models are required which will interact with the inviscid solution.

The principal equation, equation (8), is a second-order non-linear partial differential equation of the elliptic type, and the derivatives are replaced by centered finite differences. If the flow in the meridional plane is locally supersonic, the derivatives in this region should not be computed using a centered finite difference formula, since this would permit a downstream point to influence the upstream point, which is contrary to our physical knowledge of supersonic flow. Thus, strictly speaking, the technique is restricted to subsonic flow. In the analysis of the flow through turbomachinery this limitation takes two forms: if angular momentum is specified (RV_θ); $M_m < 1$, and if the flow angle is specified (β); $M_{abs} < 1$ for a stationary coordinate system and $M_{rel} < 1$ for a rotating coordinate system.

Marsh (14) suggested that the ambiguity caused by computing density and velocity could be resolved if the density were allowed to lag one iteration and the foregoing Mach number limitation could be relaxed. This would permit the computation of flow fields which contained transonic regions or supersonic patches.

This technique of lagging the density has been implemented, as described earlier, and it does improve stability at high subsonic Mach numbers. It will also permit computation of supersonic patches, if the iteration procedure is stopped when the stream function field appears to have stabilized. However, if the computation is permitted to continue, the Mach number in the supersonic region will slowly but continually increase, and will not converge to the appropriate solution.

This phenomena is not peculiar to the particular technique described in this paper, but will occur in any fixed grid stream function approach. For example, the same behavior has been observed using a relaxation technique to solve the stream function equation on the S_1 surface (15). Therefore, it appears that lagging the density one iteration, will not insure that supersonic patches may be treated.

Boundary-Layer Model

The two-layer model requires an end-wall boundary-layer calculation technique to complement the inviscid flow field computation if a realistic representation of internal flow is desired.

The technique that has been used in the computer program is an integral method based on the entrainment theory of Head (16). The two-dimensional compressible momentum-integral equation written in a streamline coordinate system is solved on each end-wall using Head's entrainment function for compressible flow as described by Summer (17), and the Ludweig-Tillman skin friction relation.

The blockage due to the boundary layer, i.e., the mass defect computed from the boundary-layer calculation, must be allowed to influence the inviscid flow computation. One manner by which this is commonly accomplished is to redefine the end-walls using the calculated displacement thickness; i.e., new fictitious physical boundaries are employed for another inviscid flow computation. Continued iteration of the two solutions will then yield the complete solution.

As described earlier, when solving equation (8) in an annular duct, the stream function values along the hub and along the casing are constants (i.e., 0 and 1.0), since each wall is essentially a streamline. An alternative to shifting the end-walls and retaining these constants for the stream function boundary values, is to change the boundary values, by an amount equal to the local mass defect of the computed boundary layer. This method is equivalent to the technique of redefining the boundary streamlines as described in the foregoing, but it does not alter the finite-difference grid, which would necessitate the repeated computation of the finite-difference coefficients. The procedure is, to solve equation (9) for $[\psi]$, calculate the end-wall boundary layers, redefine the stream function boundary values, and then solve equation (9) again. If this technique were not used, and the grid was altered each iteration, computer time would increase by a factor of 20 to 30 times.

NUMERICAL EXAMPLES

A computer program has been developed to implement the numerical procedure described in the foregoing. The program is written in FORTRAN for an IBM 370/168 with high-speed auxiliary storage, and required approximately 50 K computer words to accommodate grid sizes of 70 by 20. The computer time varies from 5 to 10 sec for the numerical examples described in the following, which all had grid sizes of approximately 30 by 8. These computer times are typical, once the matrices $[L]$ and $[U]$ have been computed for the particular grid of interest.

These examples were chosen to illustrate the technique: (a) because they are typical stationary components of centrifugal turbomachinery which are of interest to the designer and analyst; and (b) because in two of the components, the inlet and the diffuser, data was available, which indicated the flow was well-behaved and could, therefore, be used to qualify the inviscid flow technique. The third case was chosen to illustrate the flexibility of the finite-difference grid applied to a complex geometric shape, i.e., a 180-deg annular bend.

The velocity profiles which are given in the following, were obtained from an iteractive solution of the inviscid compressible flow using the finite difference technique, and a two-dimensional turbulent boundary-layer calculation which uses the technique described earlier. The boundary-layer calculation effectively provides the inviscid flow computation with a blockage.

Some of the profiles which are presented, show the results of the inviscid calculation only, and some show a combination of the inviscid and boundary-layer results. When the boundary-layer profile has been shown, it was obtained from the integral parameters of the two-dimensional boundary-layer calculation, and a power law profile faired to provide a smooth transition from one region to the other. When the inviscid profile is distorted or nonuniform, this fairing process was necessarily approximate.

Annular Inlet

The radial-to-axial annular flow inlet shown in Fig. 3(a) was designed as an experimental test rig to compare experimental data and analytical predictions (18). For this reason, there was a large amount of data available for both the inviscid flow and the end-wall boundary layers throughout the inlet. In addition, the analytical inviscid flow profiles computed by the streamline curvature method were available.

Fig. 3(b) shows the meridional velocity profiles computed at the quasi-orthogonals P-1, P-2, and P-3 [shown in Fig. 3(a)] and compares them with the experimental traverse data. The blockage due to the boundary layer is accounted for in the manner described earlier, but the boundary layer and inviscid velocity profiles have not been combined. This explains, in part, the discrepancy observed near the wall; i.e., the inviscid flow should not extend to the wall but should follow some boundary-layer velocity profile. This explanation may be seen more

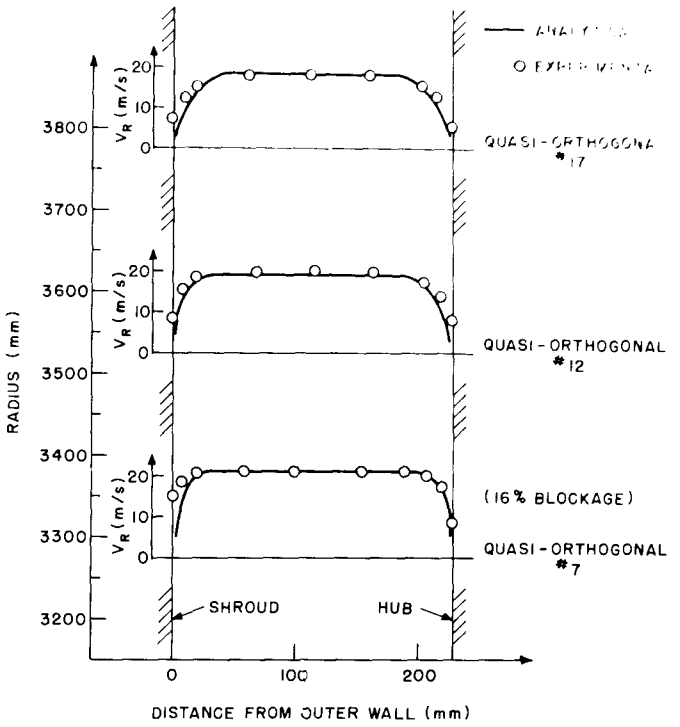

Fig. 4 Radial diffuser velocity profiles (swirl angle, α = 30 deg)

clearly in the third example where the inviscid and boundary-layer profiles are both shown in Fig. 5(b). Apart from the wall region, the agreement is very good. Also, although not shown, the agreement between the streamline curvature method and the finite-difference technique for the inviscid flow velocity profiles in this case was good.

Radial Diffuser

Fig. 4 shows the middle section of a radial diffuser which extended from an impeller tip radius of 2540 mm (10.0 in.) to an interstage return bend inlet or diffuser exit at a radius of 4318 (17.0 in.). This radial diffuser was tested extensively at Carrier (19) for a variety of compressor operating conditions, which produced a number of different diffuser inlet conditions, and thus various flow patterns. The case which is shown in Fig. 4 had uniform inlet conditions, with a swirl angle of 30 deg, and, therefore, the velocity profiles shown are uniform. In this case, the combined boundary layer and inviscid velocity profiles are plotted. The boundary-layer profile was computed from the boundary-layer parameters by assuming a power law velocity profile. The agreement with experimental data is very good.

Interstage Return Bend

The third example gives a good demonstration of the flexibility of the quasi-orthogonal grid in handling a complex geometry and flow situation. The duct shown in Fig. 5(a) is typical of the geometry used to connect one centrifugal stage to the next, although many industrial return bends have a much smaller radius of curvature on the hub to minimize the axial distance between stages.

The profiles for quasi-orthogonals Nos. 4, 15, 25, and 30 are shown in Fig. 5(b). There are two profiles, one which represents the inviscid flow, and the other the inviscid velocity profile corrected for the boundary-layer effect. As mentioned in the foregoing, the boundary-layer profiles are calculated from the computed parameters assuming a power law distribution, and then combined with the inviscid flow profile which has been calculated with the boundary-layer blockage effect.

CONCLUSIONS

This paper has described a new finite-difference technique which has been developed to permit the accurate, stable solution of the compressible flow field in the meridional plane of centrifugal turbomachinery. The method is general in the sense that complex geometric bends may be handled as easily as simple duct shapes, with third-order accuracy.

By using the double stream surface approach described by Wu (6), the complete inviscid equations of motion and continuity may be solved if sufficient information from the circumferential plane is available.

The technique has been implemented, and shown to be successful for several stationary components of centrifugal machines; an inlet bend, a radial diffuser, and an interstage return bend. In addition, although this has not been accomplished at the present time, this method is suitable for solving the inviscid flow field in rotating centrifugal turbomachinery, i.e., within the impeller. The difficulty in this case is the accurate representation of real flow effects, such as cross-flow in the boundary layers, separated flow, etc.

The technique has proved to be stable under adverse computation conditions such as extremely large curvatures and interaction with a rapidly changing end-wall boundary layer. This aspect of the technique is particularly important when the more complicated viscous flow models such as three-dimensional boundary-layer calculation, and separated flow zones are implemented, and must

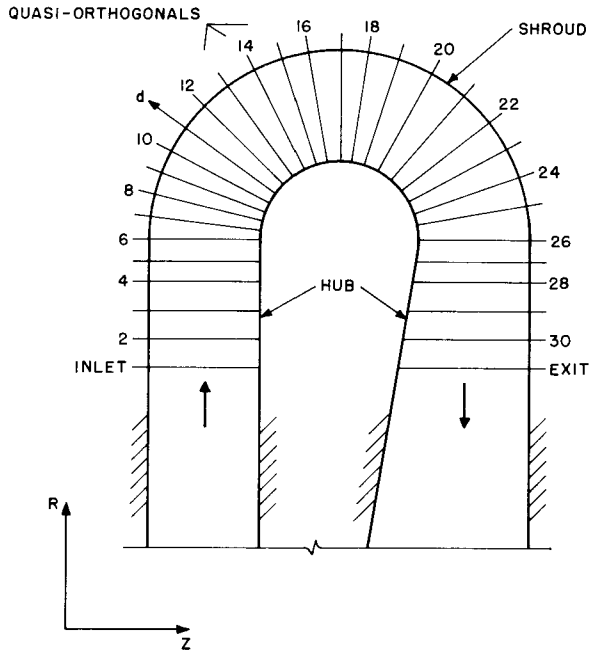

Fig. 5(a) Interstage return bend

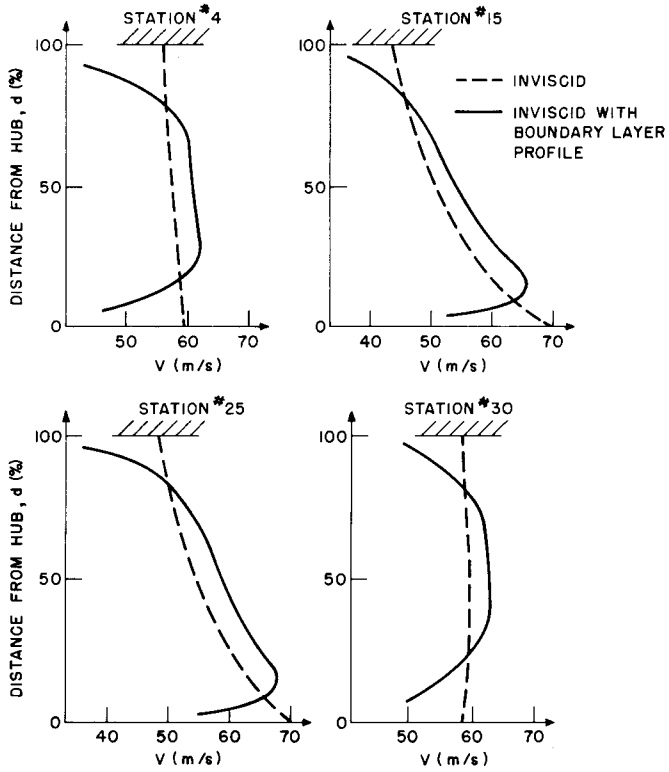

Fig. 5(b) Interstage return bend velocity profiles (flow angle = 50 deg from radial)

interact with the inviscid solution.

The availability of the quasi-orthogonal finite-difference technique will now permit concentration on the development of models for the viscous and three-dimensional flow effects in centrifugal machines. The ultimate result will be a more accurate prediction of the performance of centrifugal machines than is currently available.

ACKNOWLEDGMENTS

The author expresses his gratitude to the management at Carrier Corporation, for permission to publish this paper. The author would also like to thank Ronald H. Aungier, of the Carrier Research Division, for many helpful suggestions during the course of this work.

REFERENCES

1 Senoo, Y., and Nakase, Y., "An Analysis of Flow Through a Mixed Flow Impeller," Transactions of the ASME, Journal of Engineering for Power, Jan. 1972, pp. 43-50.

2 Novak, R. A., "The Mean Streamsheet Momentum/Continuity Solutions for Turbomachinery," ASME Fluid Dynamics of Turbomachinery, Part II, Lecture 26, 1973.

3 Stanitz, J. D., and Ellis, G. O., "Comparison of Two- and Three-Dimensional Potential Flow Solutions in a Rotating Impeller Passage," NACA TN 2806, Oct. 1952.

4 Jansen, W., "Steady Fluid Flow in a Radial Vaneless Diffuser," Transactions of the ASME, Journal of Basic Engineering, Vol. 86, Series D, 1964, pp. 607-619.

5 Dean, R. C., Jr., "On the Unresolved Fluid Dynamics of the Centrifugal Compressor," ASME "Advanced Centrifugal Compressors," 1971, pp. 1-56.

6 Wu, C.-H., "A General Theory of Three-Dimensional Flow in Subsonic and Supersonic Turbomachines of Axial-, Radial-, and Mixed Flow Types," NACA TN 2604, Jan. 1952.

7 Marsh, H., "A Digital Computer Program for the Through-Flow Fluid Mechanics in an Arbitrary Turbomachine Using a Matrix Method," National Gas Turbine Est. Report No. R. 282 1966, 7.

8 Smith, D. J. L., and Frost, D. H., "Calculation of the Flow Past Turbomachine Blades," Proceedings of the Institute of Mechanical Engineers, Vol. 184, Paper 27, 1969-1970.

9 Davis, W. R., and Millar, D. A. J., "Axial Flow Compressor Analysis Using a Matrix Method," Carleton University Report No. ME/A 73-1, 1973.

10 Davis, W. R., "A Computer Program for the Analysis and Design of Turbomachinery — Revision," Carleton University Report No. ME/A 71-5, 1971.

11 Davis, W. R., "A Matrix Method Applied to the Analysis of the Flow Past Turbomachine Blades," Carleton University Report No. ME/A 72-7, 1972.

12 Davis, W. R., and Millar, D. A. J., "A Comparison of the Matrix and Streamline Curvature Methods of Axial Compressor Analysis, From a Users Point of View," To be presented at ASME Winter Annual Meeting, 1974.

13 Wilkinson, D. H., "Stability, Convergence and Accuracy of Two-Dimensional Streamline Curvature Methods Using Quasi-Orthogonals," Proceedings of Institute of Mechanical Engineers, Vol. 184, Paper 35, 1970.

14 Marsh, H., "The Uniqueness of Turbomachinery Flow Calculations Using the Streamline Curvature and Matrix Through-Flow Methods," Journal of Mechanical Engineering Science, Vol. 13, No. 6, 1971.

15 Aungier, R. H., Private Communication, 1973.

16 Head, M. R., "Entrainment in the Turbulent Boundary Layer," R and M 3152, 1958, Aeronautical Research Council, London.

17 Sumner, W. J., and Shanebrook, J. R., "Entrainment Theory for Compressible Turbulent Boundary Layers on Adiabatic Walls," AIAA Journal, Vol. 9, No. 2, Feb. 1971, pp. 330-332.

18 Mujundar, A. S., Carrier Memorandum Report 5-1030-05, No. 3, Jan. 1971.

19 Papapanu, J. A., and Weller, P. A., Carrier Engineering Report CD1005-S1, No. 6, Feb. 1956.

APPENDIX

This derivation follows that of Wu (6) closely and is included here for completeness only.

The equation of motion, in a steady rotating coordinate system is given by

$$-\bar{W} \times (\nabla \times \bar{V}) = -\nabla I + T\nabla s \qquad (17)$$

where $\bar{W}$ is the relative velocity vector and $\bar{V}$ is the absolute velocity vector, and

$$\nabla \times \bar{V} = \nabla \times \bar{W} + 2\bar{\omega} \qquad (18)$$

where $\bar{\omega}$ is the angular velocity of the coordinate system.

For general rotational motion, the equations of motion, continuity, energy, and state may be written in cylindrical coordinates (R,θ,z) as:

1 Motion:

$$-\frac{W_\theta}{R}\left[\frac{\partial(RV_\theta)}{\partial R} - \frac{\partial W_R}{\partial \theta}\right] + W_z\left(\frac{\partial W_R}{\partial z} - \frac{\partial W_z}{\partial R}\right) = -\frac{\partial I}{\partial R} + T\frac{\partial s}{\partial R} \qquad (19a)$$

$$\frac{W_R}{R}\left[\frac{\partial(RV_\theta)}{\partial R} - \frac{\partial W_R}{\partial \theta}\right] - W_z\left(\frac{1}{R}\frac{\partial W_z}{\partial \theta} - \frac{\partial W_\theta}{\partial z}\right) = -\frac{1}{R}\frac{\partial I}{\partial \theta} + \frac{T}{R}\frac{\partial s}{\partial \theta} \qquad (19b)$$

$$-W_R\left[\frac{\partial W_R}{\partial z} - \frac{\partial W_z}{\partial R}\right] + W_\theta\left(\frac{1}{R}\frac{\partial W_z}{\partial \theta} - \frac{\partial W_\theta}{\partial z}\right) = -\frac{\partial I}{\partial z} + T\frac{\partial s}{\partial z} \qquad (19c)$$

2 Continuity:

$$\frac{1}{R}\frac{\partial}{\partial R}\left(\rho R W_R\right) + \frac{1}{R}\frac{\partial}{\partial \theta}\left(\rho W_\theta\right) + \frac{\partial}{\partial z}\left(\rho W_z\right) = 0 \quad . \qquad (20)$$

3 Energy:

$$T\frac{Ds}{Dt} = Q \quad . \qquad (21)$$

4 State (perfect gas);

$$P = \rho R_g T \qquad (22)$$

In order to solve the steady three-dimensional flow in a relatively simple manner, an approach is taken to obtain the three-dimensional solution by an appropriate combination of mathematically two-dimensional flows on essentially two different kinds of relative stream surface. The first kind of relative stream surface is one whose intersection with the Z-plane at some location (i.e., inlet) is a circular arc. The second kind of relative stream surface is one whose intersection with the Z-plane at some location in the region to be considered forms a radial line. These surfaces are called the S_1 and S_2 surfaces, respectively. In this development, we will consider the S_2 surface defined by

$$S_2(R,\theta,z) = 0 \quad , \qquad (23)$$

It is convenient to consider the unit vector, $\bar{n}$, normal to the surface, which is related to S_2 by

$$n_R\, dR + n_\theta\, d\theta + n_z\, dz = 0 \quad . \qquad (24)$$

The vector, $\bar{n}$, is perpendicular to the relative velocity, $\bar{W}$, so that

$$\bar{n} \cdot \bar{W} = 0 \quad . \qquad (25)$$

Equations (23), (24), and (25) will now be used to eliminate the independent variable, θ; i.e., any quantity, q, on S_2 is now considered as

$$q = q\left[R, z, \theta(R,z)\right] .$$

Accordingly, on S_2,

$$\frac{\bar{\partial} q}{\partial R} = \frac{\partial q}{\partial r} - \frac{n_R}{n_\theta} \frac{1}{R} \frac{\partial q}{\partial \theta} \quad , \tag{26a}$$

$$\frac{\bar{\partial} q}{\partial z} = \frac{\partial q}{\partial z} - \frac{n_z}{n_\theta} \frac{1}{R} \frac{\partial q}{\partial \theta} \quad , \tag{26b}$$

where the operator $\bar{\partial}(\ )$ is used to denote the rate of change of any quantity, q, on S_2, with respect to R or z, with the other held constant.

The continuity equation thus becomes

$$\frac{1}{R} \frac{\bar{\partial}(\rho W_R R)}{\partial R} + \frac{\bar{\partial}(\rho W_z)}{\partial z} = \rho . C(R, z) \quad , \tag{27}$$

where

$$C(R, z) = - \frac{1}{n_\theta R} \left(n_R \frac{\partial W_R}{\partial \theta} + n_\theta \frac{\partial W_\theta}{\partial \theta} + n_z \frac{\partial W_z}{\partial \theta} \right) .$$

The equations of motion in the three perpendicular directions become

$$- \frac{W_\theta}{R} \left[\frac{\bar{\partial}(RV_\theta)}{\partial R} + W_z \left(\frac{\bar{\partial} W_R}{\partial z} - \frac{\bar{\partial} W_z}{\partial R} \right) \right] = - \frac{\bar{\partial} I}{\partial R} + T \frac{\bar{\partial} S}{\partial R} + F_R , \tag{28a}$$

$$\frac{W_R}{R} \frac{\bar{\partial}(RV_\theta)}{\partial R} + \frac{W_z}{R} \frac{\bar{\partial}(RV_\theta)}{\partial z} = F_\theta \left[\text{or } F_\theta R = \frac{D(RV_\theta)}{Dt} \right] , \tag{28b}$$

$$-W_R \left(\frac{\bar{\partial} W_R}{\partial z} - \frac{\bar{\partial} W}{\partial R} \right) - \frac{W_\theta}{R} \frac{\bar{\partial}(RV_\theta)}{\partial z} = - \frac{\bar{\partial} I}{\partial z} + T \frac{\bar{\partial} S}{\partial z} + F_z , \tag{28c}$$

where $\bar{F}$ is a vector having the units of force per unit mass of gas, defined by

$$\bar{F} = - \frac{1}{n_\theta R} \left(\frac{\partial h}{\partial \theta} - T \frac{\partial s}{\partial \theta} \right) \bar{n} \quad .$$

Since the vector, $\bar{F}$, is normal to the S_2 surface

$$\bar{F} \cdot \bar{W} = 0 \tag{29}$$

For convenience, the bar over the partial derivative operator will be omitted in the remainder of the development.

By the use of an integrating factor, b, the continuity equation, equation (27), may be put in the form

$$\frac{\partial (Rb\rho W_R)}{\partial R} + \frac{\partial (Rb\rho W_z)}{\partial z} = 0 , \tag{30}$$

which is the necessary and sufficient condition that a stream function, ψ, exist and

$$\frac{\partial \psi}{\partial R} = Rb\rho W_z \quad , \tag{31a}$$

$$\frac{\partial \psi}{\partial z} = - Rb\rho W_R \quad . \tag{31b}$$

It may be shown that b is proportional to the angular thickness of a thin stream sheet whose mean surface is the stream surface, S_2, and whose variable circumferential thickness is equal to Rb.

The equations of motion may be combined using equation (29), to give

$$\frac{DI}{Dt} = T \frac{Ds}{Dt} \quad . \tag{32}$$

If equation (31) is substituted into the radial and axial components of the equation of motion, i.e., equations (28a) and (28c), the following equations will result:

$$\frac{\partial^2 \psi}{\partial R^2} + \frac{\partial^2 \psi}{\partial z^2} = q(R, z) - \frac{Rb\rho}{W_R} \left[- \frac{\partial I}{\partial R} + T \frac{\partial s}{\partial R} + F_R + \frac{W_\theta}{R} \frac{\partial (RV_\theta)}{\partial R} \right] , \tag{33a}$$

and

$$\frac{\partial \psi}{\partial R^2} + \frac{\partial^2 \psi}{\partial z^2} = q(R, z) + \frac{Rb\rho}{W_z} \left[- \frac{\partial I}{\partial z} + T \frac{\partial s}{\partial z} + F_z + \frac{W_\theta}{R} \frac{\partial (RV_\theta)}{\partial z} \right] \tag{33b}$$

where

$$q(R, z) = \frac{\partial \psi}{\partial R} \cdot \frac{\partial (\ln b\rho R)}{\partial R} + \frac{\partial \psi}{\partial z} \cdot \frac{\partial (\ln b\rho)}{\partial z} .$$

For concisness, these may be written

$$\nabla^2(\psi) = q(R, z) + \xi_i , \qquad \text{for } i = 1, 2 \tag{34}$$

where

$$\xi_1 = - \frac{Rb\rho}{W_R} \left[- \frac{\partial I}{\partial R} + T \frac{\partial s}{\partial R} + F_R + \frac{W_\theta}{R} \frac{\partial (RV_\theta)}{\partial R} \right]$$

and

$$\xi_2 = \frac{Rb\rho}{W_z} \left[- \frac{\partial I}{\partial z} + T \frac{\partial s}{\partial z} + F_z + \frac{W_\theta}{R} \frac{\partial (RV_\theta)}{\partial z} \right]$$

Equation (34) will be referred to as the stream function equation or the principal equation.